Theoretical Consideration of Nondestructive Testing by use of Vertical Magnetization and Magneto-Optical Sensor

Jinyi Lee*
Division of Information & Control Measurement Engineering, Chosun University, 375 Seosuk-dong, Dong-gu, Gwangju 501-759, Korea
Tetsuo Shoji
Fracture Research Institute, Tohoku University, Aoba-01, Aramaki-Aza, Aoba-ku, Sendai 980-8579, Japan
Dowon Seo
Department of Mechanical Design, Chonbuk University, Duckjin 1-664-14, Chonju 561-756, Korea

This paper describes a new magnetization method for non-destructive testing with magneto-optical sensor (denoted as MO sensor) which have the following characteristic ; high observation sensitivity, independence of the crack orientation, and precise imaging of a complex crack geometry such as multiple cracks. When a magnetic field is applied normally to the surface of a specimen which is significantly larger than its defects, approximately the same magnetic charge per unit area occurs on the surface of the specimen. If there is a crack in the specimen, magnetic charge per unit area has the same value at the bottom of the crack. The distribution of the vertical component of the magnetic flux density, B_Z, is almost uniform over the no-crack area (denoted as $B_{Z,BASE}$), while the magnetic flux density is smaller in the surroundings of the crack (denoted as $B_{Z,CRACK}$). If $B_{Z,BASE}$ is a bit larger than the saturated magnetic flux density of the MO sensor (B_S), then small magnetic domains occur over the crack area and a large domain over the non-crack area because $B_{Z,CRACK}$ is smaller than B_S.

Key Words : NDT (Non-Destructive Testing), MO Sensor (Magneto-Optical Sensor), Leakage Magnetic Flux (LMF), Lift-off, Faraday Effect, Vertical Magnetization, Dipole Model

Nomenclature

B_S : Saturated magnetic flux density of the MO sensor
$B_{Z,BASE}$: Magnetic flux density to the vertical direction of the specimen over the no-crack area
$B_{Z,CRACK}$: Magnetic flux density to the vertical direction of the specimen on the crack area
B_Z, $B_{Z,TOTAL}$: Magnetic flux density to the vertical direction of the specimen
l_C, w_C, d_C : Length, width and depth of a crack
l_S, w_S : Length and width of a specimen
θ_C : Angle between the longitudinal direction of a crack and the x-direction
x : Longitudinal direction of a specimen
y : Lateral direction of a specimen
z : Vertical direction to the specimen
z_{lift} : lift-off from surface of a specimen to the MO sensor

* Corresponding Author,
E-mail : jinyilee@mail.chosun.ac.kr
TEL : +82-62-230-7101; **FAX** : +82-62-230-7101
Division of Information & Control Measurement Engineering, Chosun University, 375 Seosuk-dong, Dong-gu, Gwangju 501-759, Korea. (Manuscript **Received** September 29, 2003; **Revised** January 2, 2004)

1. Introduction

Nondestructive testing (NDT) using the mag-

netic domain of a magneto-optical (MO) sensor was suggested as a method of inspecting cracks (Fitzpatrick et al., 1993 ; Ishihara et al., 1996 ; Lee et al., 1997, 1998, 1999a, 1999b, 2000 ; Lim et al., 2002). The advantages of NDT using the magnetic domain of an MO sensor is a method that enables detecting cracks without contact ; thus, it isn't needed to remove the paint, high spatial resolution could be obtained by transacting the distribution of leakage magnetic flux around the crack to the MO sensor, and high speed testing could be possible. On the other hand, remote detecting is possible using the density of domain walls and optical permeability (Lee et al., 1999b). Furthermore, the MO sensor could not be bent due to brittleness but could be grinded so that a new NDT method, which senses micro-cracks in structures having a curved surface such as the inner wall of piping, introduced (Lee et al., 1998 ; Lim et al., 2002). Especially, high sensitivity is the characteristic of the NDT method using a narrow MO sensor having the vertical component of leakage magnetic flux, which is effective in detecting environmentally associated cracks in curved structures. The magnetizing method on these NDT using the MO sensor uses the Yoke method (Ishihara et al., 1996 ; Lee et al., 1997, 1998, 1999a, 1999b, 2000 ; Lim et al., 2002), which is based on the principle of occurring a large magnetic flux to the specimen using a closed circuit of magnetic flux. However, the Yoke method that uses a closed circuit of magnetic flux is significantly dependent upon the angle formed between the crack and magnetizing direction. Furthermore it is difficult to detect and interpret the intersecting cracks because that adjacent cracks affect each other. In this study, a new magnetizing method, which is conceptually different from the ones introduced previously, is introduced and is discussed theoretically. This method enables making image processing simple by granting the full characteristic of an MO sensor transacting the spatial distribution of magnetic flux while not depending on the direction of cracks and granting a lower density of domain wall in the areas with no cracks and a higher density of domain wall in the areas with cracks. Furthermore, the result of theoretical discussion was compared with the result of an experiment conducted using an actual structure.

2. Theoretic Discussion on Leakage Magnetic Flux

2.1 Leakage magnetic flux due to horizontal magnetization

Figure 1 is a schematic of leakage magnetic flux due to a closed circuit of magnetic flux using the Yoke method that is usually used for crack detecting. When a core is wrapped with coil and AC or DC is inputted, the core is magnetizing in which both ends functioning as opposite poles. Magnetic flux is occurred inside of the specimen horizontally to the surface of the specimen by placing a ferromagnetic specimen at each end of poles, and leakage magnetic flux is appeared by the discontinuity such as cracks.

Figure 2 is a dipole model of a crack and coordinate system. The size of a crack is the

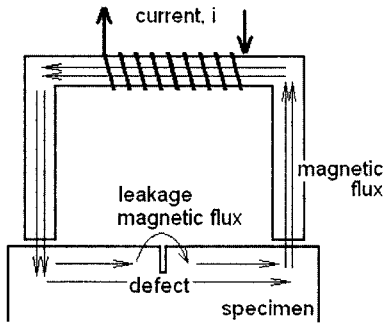

Fig. 1 Leakage magnetic flux

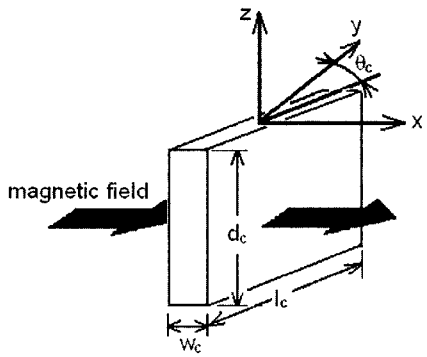

Fig. 2 Dipole model of crack

length of l_C, the width of w_C and the depth of d_C. The x-y plane would represent the surface of the specimen, and the z-direction would represent the vertical direction to the surface of a specimen. When the magnetizing direction due to a Yoke's magnetizer is considered as the x-direction, the vertical direction of the x-z plan would be the y-direction. Furthermore, the direction of crack length is rotated by θ_C in the y-direction.

When $\theta_C=0$, the direction of crack length is the same as the y-direction. The z-direction component of the leakage magnetic flux density B, i.e., $B_Z(\theta_C=0)$, can be expressed as the following equation (Minkov et al., 2000; Mukae et al., 1988; Lee et al., 2000).

$$B_Z(\theta_C=0)=\frac{m}{4\pi}\int_{-l_c/2-y}^{l_c/2-y}\int_0^{d_c}\frac{z+u}{\{(x+w_C/2)^2+y^2+(z+u)^2\}^{3/2}}dudy - \frac{m}{4\pi}\int_{-l_c/2-y}^{l_c/2-y}\int_0^{d_c}\frac{z+u}{\{(x-w_C/2)^2+y^2+(z+u)^2\}^{3/2}}dudy \quad (1)$$

Here, m is the magnetic charge per unit area, and u is the distance between the dipole and the surface plane of the specimen.

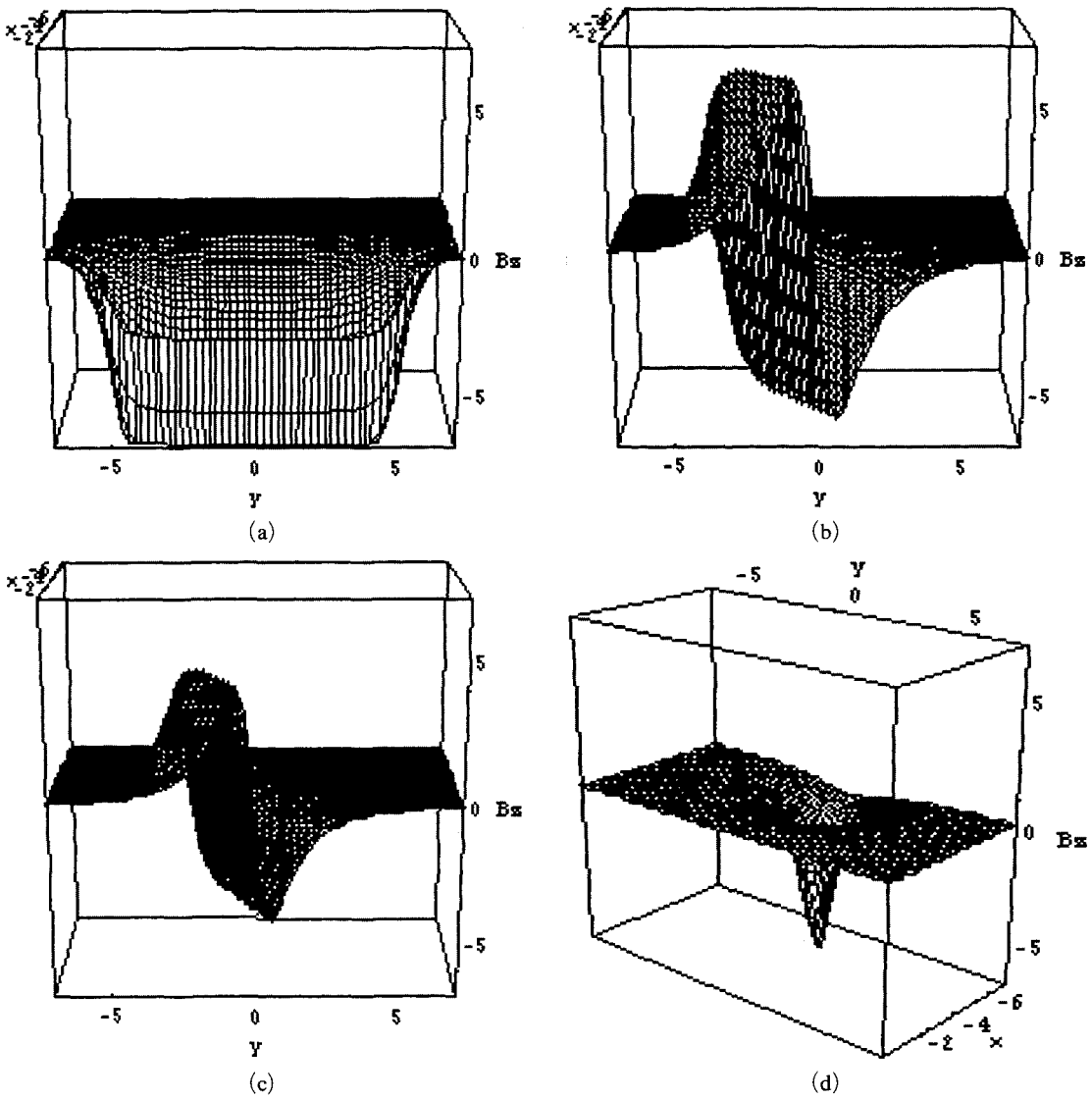

Fig. 3 Distribution of B_Z by horizontal magnetization (a) $\theta_C=0$, (b) $\theta_C=\pi/4$, (c) $\theta_C=\pi/3$, (d) $\theta_C=\pi/2$

In the case of $\theta_C=\pi/2$, B_Z according to Eq. (1) can be calculated by replacing w_C and l_C. Furthermore, if w_C is significantly smaller than d_C, l_C, in the case of $0\leq\theta_C<\pi/2$, B_Z can be calculated with Eq. (2).

$$B_Z=\frac{m\cos\theta_C}{4\pi}\int_{-l_C/2-y'}^{l_C/2-y'}\int_0^{d_C}\frac{z+u}{\{(x'+w_C/2)^2+y'^2+(z+u)^2\}^{3/2}}dudy' - \frac{m\cos\theta_C}{4\pi}\int_{-l_C/2-y'}^{l_C/2-y'}\int_0^{d_C}\frac{z+u}{\{(x'-w_C/2)^2+y'^2+(z+u)^2\}^{3/2}}dudy' \quad (2)$$

Here, x', y' can be shown with Eq. (3).

$$x'=\sqrt{x^2+y^2}\cos\left[\frac{\pi}{2}-\theta_C-\tan^{-1}\left(\frac{y}{x}\right)\right]$$
$$y'=\sqrt{x^2+y^2}\sin\left[\frac{\pi}{2}-\theta_C-\tan^{-1}\left(\frac{y}{x}\right)\right] \quad (3)$$

Using the Eqs. (2) and (3), the distribution of leakage magnetic flux density B_Z on the x-y plane, when the lift-off, z_C is 0.5 mm, is calculated at the condition of (a) $\theta_C=0$, (b) $\theta_C=\pi/4$, and (c) $\theta_C=\pi/3$ and (d) $\theta_C=\pi/2$ respectively as shown in Fig. 3, where the size of a crack is w_C=0.5 mm, l_C=10 mm, and d_C=1.5mm. The region of calculating is x=−7 mm=−0.1 mm and y=−7 mm~7 mm. The magnetic charge per unit area is assumed as constant, $m/4\pi=10$. As shown in Fig. 3(a), the length direction of crack is vertical to the magnetizing direction, ($\theta_C=0$) becomes largest in spite of the same sized crack. As shown in Figs. 3(b) and (c), the overall leakage magnetic flux density became smaller according to the increasing angle, θ_C. Furthermore, in the case of $\theta_C=\pi/2$, it is suggesting the low probability of detecting cracks because that information from both ends of a crack only appear as shown in Fig. 3(d). It means that there is a close relationship between the longitudinal direction of a crack and magnetizing direction.

2.2 Theoretical consideration on horizontal magnetization

Fig. 4 shows the principle of a new magnetizing method. As shown in Fig. 4(a), when magnetic field is applied to the vertical direction to the surface of a specimen sufficiently larger than a crack ($l_S \gg l_C$, $w_S \gg w_C$, l_S=length of specimen/ w_S=width of specimen), the magnetic charge per unit area, m, having almost uniform occurs on the surface of the specimen. When a crack is present here as shown in the A-A' surface of Fig. 4(b), m is present in the bottom of the crack. Thus, the distribution of magnetic flux density B_Z on the x-y plane with lift-off, z_{lift}, was $B_{Z,BASE}$ as shown in Fig. 4(c), which is almost uniform in the areas with no crack. However, the lift-off is $z_{lift}+d_C$ on top of a crack, showing a low magnetic flux density $B_{Z,CRACK}$. Here, $B_{Z,BASE}$ can be controlled by controlling the input current of the magnetizer. If $B_{Z,BASE}$ is set slightly larger than B_S (saturated magnetic flux density of MO sensor), $B_{Z,CRACK}$ would be lower than B_S; thus, the transaction of crack would occur. Furthermore, the probability of detecting cracks according to this magnetizing method would be depend only the area ($W_C \times l_C$) and location (d_C) of cracks in the bottom and not be related with the angle formed by length direction and y-direction of the crack.

In order to derive a general equation based on this principle, the model shown in Fig. 5 could

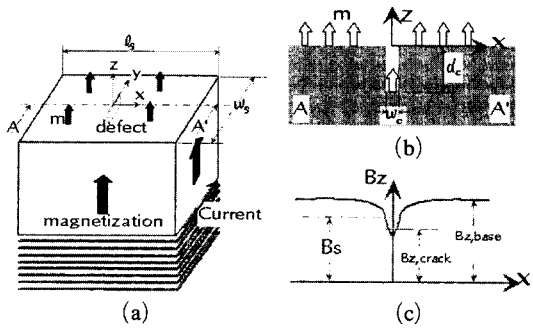

Fig. 4 Principle of the new magnetization method (a) Coordinate (b) Magnetic charge per unit area on the x-y plane (c) Distribution of magnetic flux

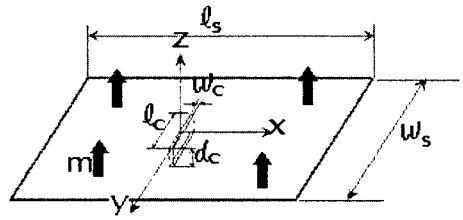

Fig. 5 Modeling of the crack and vertical magnetization

Equation (14) expresses the unknown acceleration vector of particle 3 in terms of the acceleration vectors of the other primary particles which eliminates the constraint Eqs. (4.4) to (4.7). Equation (14) can be put in the more convenient form

$$\begin{aligned}\ddot{\mathbf{r}}_3 = &(1-\mu-\tau+\lambda\tilde{\mathbf{r}}_{4,2})\ddot{\mathbf{r}}_1 \\ &+(\tau-\lambda\tilde{\mathbf{r}}_{4,1})\ddot{\mathbf{r}}_2+(\mu+\lambda\tilde{\mathbf{r}}_{2,1})\ddot{\mathbf{r}}_4\end{aligned} \tag{15}$$

Substituting the derived acceleration vector of particle 3 from Eq. (15) into Eqs. (5) and (6), then the differential equations of motion take the modified form

$$\begin{aligned}\mathbf{R} = &\{\bar{m}_1+\bar{m}_3(1-\mu-\tau+\lambda\tilde{\mathbf{r}}_{4,2})\}\ddot{\mathbf{r}}_1 \\ &+\{\bar{m}_2+\bar{m}_3(\tau-\lambda\tilde{\mathbf{r}}_{4,1})\}\ddot{\mathbf{r}}_2 \\ &+\{\bar{m}_4+\bar{m}_3(\mu+\lambda\tilde{\mathbf{r}}_{2,1})\}\ddot{\mathbf{r}}_4+2\lambda\bar{m}_3\dot{\tilde{\mathbf{r}}}_{2,1}\dot{\mathbf{r}}_{4,1}\end{aligned} \tag{16}$$

$$\begin{aligned}G_1 = &\{A_1+A_3(1-\mu-\tau+\lambda\tilde{\mathbf{r}}_{4,2})\}\ddot{\mathbf{r}}_1 \\ &+\{A_2+A_3(\tau-\lambda\tilde{\mathbf{r}}_{4,1})\}\ddot{\mathbf{r}}_2 \\ &+\{A_4+A_3(\mu+\lambda\tilde{\mathbf{r}}_{2,1})\}\ddot{\mathbf{r}}_4+2\lambda A_3\dot{\tilde{\mathbf{r}}}_{2,1}\dot{\mathbf{r}}_{4,1}\end{aligned} \tag{17}$$

Equations (16) and (17) in addition to the constraint Eqs. (4.1) to (4.3) represent the equations of motion of a single floating rigid body in spatial motion. It can be solved at every time step to determine the unknown acceleration components of particles 1, 2, and 4. Consequently, Eq. (15) can be used to determine the acceleration components of particle 3. The acceleration components of the particles are integrated numerically, knowing their Cartesian coordinates and velocities at a certain time step, to determine the positions and velocities for the next time step. The translational motion of the particles determines completely the translational and rotational motion of the rigid body. If the rigid body is rotating about a fixed point, then particle 1 may be located at the centre of this joint. In this case, Eq. (17) and Eqs. (4.1) to (4.3) are used to solve for the unknown Cartesian accelerations of particles 2 and 4. Equation (16) can be solved to determine the unknown reaction forces at the joint.

If the rigid body is rotating about a fixed axis, then particles 1 and 2 can be located along the axis of the joint to define its direction. The projection of the moments in Eq. (17) along the direction of the axis of the revolute joint in addition to the constraint Eqs. (4.2) and (4.3) can be used to determine the unknown acceleration vector of particle 4. Then, Eq. (16) may be used to get the reactions at the axis of the revolute joint.

2.4 Equations of motion of a serial chain of rigid bodies

Figure 3 shows a serial chain of N rigid bodies with the equivalent system of (3N+1) particles where connected particles are unified from both bodies. For the last body "N" in the chain, the equations of motion are derived in a similar way as Eq. (17) and Eqs. (4.1) to (4.3) of a single rigid body. The angular momentum equation takes the form

$$\begin{aligned}G_{3N-2} = &\{A_{3N-2}+A_{3N}(1-\mu_N-\tau_N+\lambda_N\tilde{\mathbf{r}}_{3N+1,3N-1})\}\ddot{\mathbf{r}}_{3N-2} \\ &+\{A_{3N-1}+A_{3N}(\tau_N-\lambda_N\tilde{\mathbf{r}}_{3N+1,3N-2})\}\ddot{\mathbf{r}}_{3N-1} \\ &+\{A_{3N+1}+A_{3N}(\mu_N+\lambda_N\tilde{\mathbf{r}}_{3N-1,3N-2})\}\ddot{\mathbf{r}}_{3N+1} \\ &+2\lambda_N A_{3N}\dot{\tilde{\mathbf{r}}}_{3N-1,3N-2}\dot{\mathbf{r}}_{3N+1,3N-2}\end{aligned} \tag{18}$$

where

$$A_{3N}=\bar{m}_{3N}\tilde{\mathbf{r}}_{3N,3N-2}+\sum_{\substack{i=3N-1\\ i\neq 3N}}^{3N+1}\frac{1}{4}m_{3N,i}\tilde{\mathbf{r}}_{i,3N-2}$$

$$\bar{m}_{3N}=m_{3N}+\sum_{\substack{i=3N-2\\ i\neq 3N}}^{3N+1}\frac{1}{4}m_{3N,i}$$

where G_{3N-2} is the sum of the moments of the external forces and force couples acting on body N with respect to the location of particle 3N−2. The acceleration equations of the distance constraint between primary particles belonging to body N are given as

$$\begin{aligned}&\mathbf{r}^T_{3N-2,3N-1}\ddot{\mathbf{r}}_{3N-2}+\mathbf{r}^T_{3N-1,3N-2}\ddot{\mathbf{r}}_{3N-1} \\ &=-\dot{\mathbf{r}}^T_{3N-1,3N-2}\dot{\mathbf{r}}_{3N-1,3N-2}\end{aligned} \tag{19.1}$$

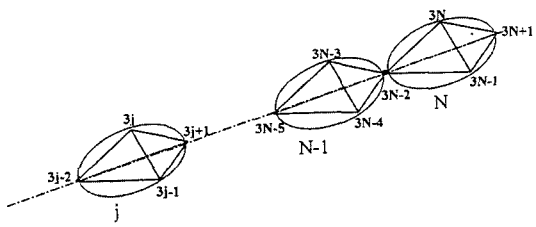

Fig. 3 Serial chain of N rigid bodies with an equivalent system of primary particles

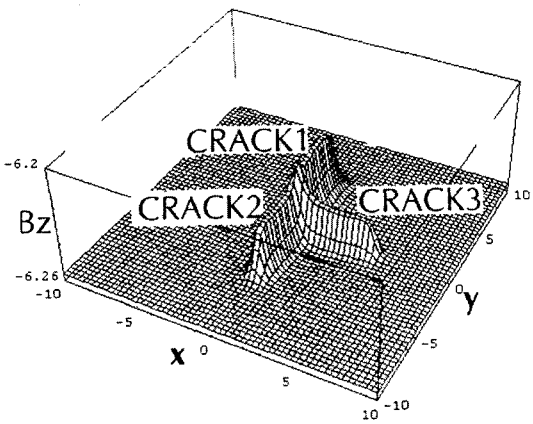

Fig. 8 Distribution of B_z on the multiple cracks by vertical magnetization

calculating the distribution of magnetic flux density $B_{z,TOTAL}$ when $m/4\pi=-1$ (for easier to look at, (−) values were taken), $x=-10$ mm~10 mm, and $y=-10$ mm~10 mm using Eq. (7). By hypothesizing a sample with the width (w_S) of 180 mm and length (l_S) of 260 mm, the lift-off (z_C) was calculated as 0.5 mm. From this calculation, we could tell that the detecting sensitivity was not affected by the length direction, θ_C (or magnetizing direction) of the crack present on the x-y plane.

3. Specimens and Magnetizer

The specimen and magnetizer are explained in order to verify the effectiveness of the vertical magnetization method. Table 1 shows the specimen. S1 is a rectangular shape of crack which is machined artificially using an electro-discharge machining in an A508 sample. S2 shown in Fig. 9 is the brittle fatigue specimen prepared using A533B (Oh, 2002) and was fractured using the 3-point bending test. Micro-brittle fatigue cracks present around the fractured surface were sensed. Here, Crack 1 shows the crack with narrow left side and wide right side. However, the crack progressed from the left to the right side. And the slope was present toward the top direction in the figure. Furthermore, there was crack with almost no width between Crack 1 and Crack 2. The specimen surface was grinded to remove any unevenness.

Table 1 Specimens

No.	Materials	Type of Cracks	Introduction of a Crack	Size of Specimen (mm)
S1	A508	Slit	Electric Discharge	$108w_S \times 260l_S \times 20t_S$*
S2	A533B-steel	Brittle Fatigue	Large Three-point Bend	$160w_S \times 350l_S \times t_S$*

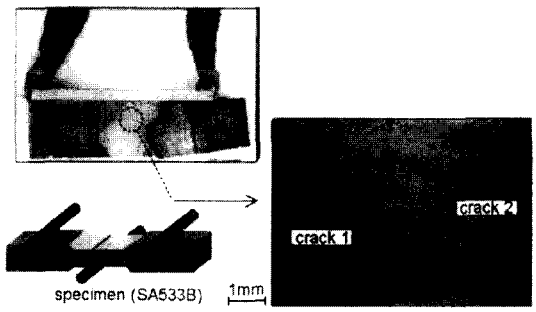

Fig. 9 Brittle fatigue cracks

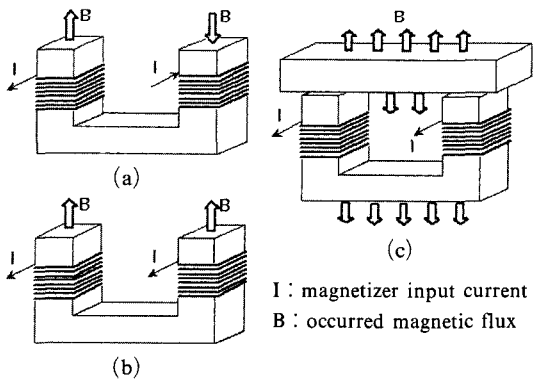

Fig. 10 Generation of the magnetic field by new method for the flat specimen

On the other hand, vertical magnetization could be realized according to the simple composition as shown in Fig. 10. A magnetic field (Fig. 10 (b)) in the same direction was occurred at each end of the coil by inputting the current to the opposite direction at the one end of Yoke magnetizer coil as shown in Fig. 10(a). When the specimen was placed on the each poles of magnetizer, the flow of overall magnetic flux is like that from two magnets with a shape of short bar as shown in Fig. 10(c). Therefore, the specimen was magnetized toward the vertical direction at the sur-

face, and intensity of the magnetic field could be controlled by the input current. Furthermore, the distribution of magnetic flux density on the surface of a specimen became uniform as the thickness of the specimen increased. This intensity was sufficiently larger than the saturated magnetic field of an MO sensor so that the vertical magnetizing method examined in this study would be effective for thick iron plates actually used.

4. Results and Discussion

Figure 11 shows the result (Fig. 11(a)) of detecting S1 (Fig. 11(b)) using an MO sensor when a vertical magnetic field was applied to a specimen according to the described magnetizing structure and specimen arrangement. This result suggests that the conclusion of the theoretical discussion in Fig. 6, in which the width and length of a crack could be obtained with the method of vertical magnetization regardless of the length direction of a crack, is correct in the case of an opened crack.

Figure 12 shows the result of detecting using an MO sensor after a vertical magnetic field was applied to multiple cracks of S2. Where the dotted lines mean the position and the size of cracks which was observed from a surface of a specimen. When the amount of magnetic charge per unit area, m was maximized by maximizing the input current (10A) to the magnetizer, the information on crack could be obtained as Fig. 12(a) because

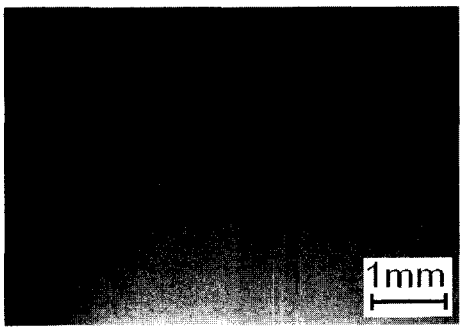

(a) Magneto-optical image

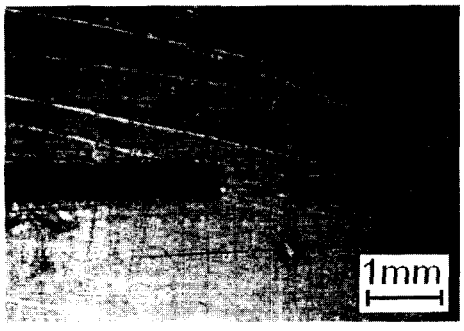

(b) Specimen

Fig. 11 Magneto-optical image of a simple crack with a vertical magnetization

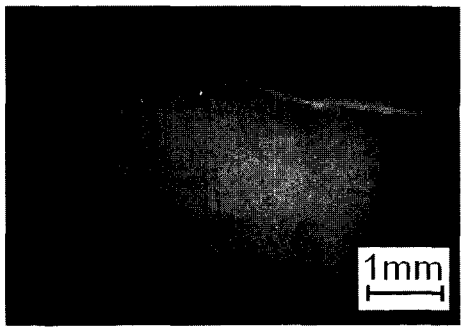

(a) 10A

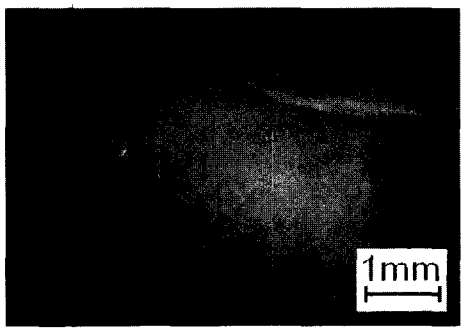

(b) 4.1A

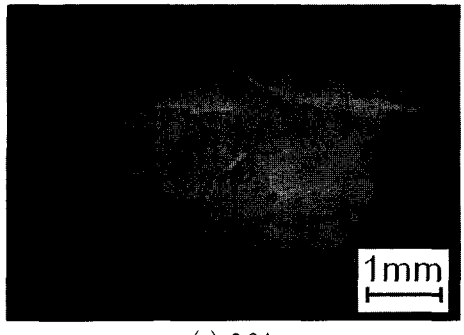

(c) 3.0A

Fig. 12 Magneto-optical images of multiple cracks with a vertical magnetization

inversion of magnetic poles occurs near the specimen surface since the depth and direction of crack do not parallel to the surface magnetizing direction of the specimen. On the other hand, Fig. 12(b) shows information of the crack when the distribution of leakage magnetic field around the crack was transacted to the MO sensor when the input current was lowered to 4.1A. It is expanded toward the top direction along with the information of Crack 2 as information from Crack 1 progressed toward the right side, suggesting that the depth of the right side is deeper in spite of the fact that the width of Crack 1 at the right side is larger (Fig. 9) and that Crack 1 and Crack 2 are sloped toward the upper side. This trend became more apparent as the input current was lowered to 3.0A as shown in Fig. 12(c). Information of another crack was shown between Crack 1 and Crack 2, suggesting the presence of inner crack. This trend disappeared as the input current became 0A. These results suggest that as in the theoretical discussion in Fig. 8, the length direction of a crack on the specimen surface is not affected with the new vertical magnetizing method, and the width, direction, depth, and slope could be predicted for multiple cracks actually seen frequently compared with the previous horizontal magnetizing method.

5. Conclusion

New magnetization method for NDT using an MO sensor was introduced and discussed in this study. According to the theoretical discussion and experiment, the following are the advantages of the new detecting method for the opened cracks using an MO sensor and the vertical magnetizing method, compared with the horizontal magnetizing method as a yoke; (1) image processing and the interpretation are easy since an MO sensor could transact only the crack information, (2) the length direction of crack does not affect the detecting ability, and (3) the quantitative analysis of crack width and length is easy since cracks do not affect each other in case of multiple cracks. Furthermore, this method was also effective for the structures such as a thick iron plate when the vertical magnetizing method was applied to micro brittle fatigue cracks present on large brittle specimens prepared with A533B.

References

Fitzpatrick, G. L., Thome, D. K., Skaugset, R. L., Shih, E. Y. C. and L. Shih, W. C., 1993, "Magneto-Optic/Eddy Current Imaging of Aging Aircraft-A New NDI Technique," Materials *Evaluation*, Vol. 51, No. 12, pp. 1402~1407.

Ishihara, M., Sakamoto, T., Haruna, K., Nakamura, N., Machida, K. and Asahara, Y., 1996, "Advanced Magnetic Flux Leakage Testing System Using Magneto-Optical Film," *Journal of the Japanese Society for Nondestructive Inspection*, Vol. 45, No. 4, pp. 283~289.

Lee, J. and Shoji, T., 1999a, "Developtment of a NDI System using the Magneto-Optical Method-Development of the Magneto-Optical Inspection System," *Journal of the Japanese Society for Non-Destructive Inspection*, Vol. 48, No. 3, pp. 165~171.

Lee, J. and Shoji, T., 1999b, "Development of a NDI System using the Magneto-Optical Method-Remote Sensing using the Novel Magneto-Optical Inspection System," *Journal of the Japanese Society for Non-Destructive Inspection*, Vol. 48, No. 4, PP. 231~236.

Lee, J., Lee, H., Shoji, T. and Minkov, D., 1998, *Electromagnetic Nondestructive Evaluation (II)*, IOS Press, Amsterdam, pp. 49~57.

Lee, J., Lyu, S. and Nam, Y., 2000, "An Algorithm for the Characterization of Surface Crack by Use of Dipole Model and Magneto-Optical Non-Destructive Inspection System," *KSME International Journal*, Vol. 14, No. 10, pp. 1072~1080.

Lee, J., Shoji, T. and Najib, N., 1997, "Development of the Crack Inspection System by use of Laser and Leakage Magnetic Flux," *Proceedings of Symposium on Optical NDT Methods for Surface Flaw Detection*, Tokyo, pp. 55~62.

Lim, J., Lee, H., Lee, J. and Shoji, T., 2002, "Application of a NDI Method Using Magneto-Optical Film for Micro-Cracks," *KSME International Journal*, Vol. 16, No. 5, pp. 591~598.

Minkov, D., Lee, J. and Shoji, T., 2000, "Improvement of the Dipole Model of a Surface Crack," *Materials Evaluation*, Vol. 58, No. 5, pp. 661~666.

Mukae, S., Kotoh, M. and Nishio, K., 1988, "Investigation of Quantification for Defect and Effect of Factors Affecting Leakage Flux Density in Magnetic Leakage Flux Testing Method," *Journal of the Japanese Society for Non-Destructive Inspection*, Vol. 37, No. 11, pp. 885~894.

Oh, D., 2002, "Ductile Fracture Behavior of AS4P Under Mixed Mode (I/II) Loading," *KSME International Journal*, Vol. 16, No. 4, pp. 476~484.